Publishing House
AKAPIT

COMPUTER METHODS IN MATERIALS SCIENCE

Informatyka w Technologii Materiałów

Vol. 11, 2011, No. 2

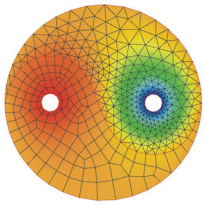

CRACKLING NOISE IN A DISCRETE ELEMENT MODEL OF SINGLE CRACK PROPAGATION

GÁBOR TIMÁR*, FERENC KUN

Department of Theoretical Physics, University of Debrecen
P.O. Box 5, H-4010 Debrecen, Hungary
**Corresponding author: tgabor@phys.unideb.hu*

Abstract

We study the crackling noise emerging during single crack propagation obtained by discrete element modelling (DEM) in a specimen under three-point bending conditions. Analyzing temporal and spatial correlations of local breakings we show that the crack proceeds in bursts, which are characterized by power law distributions of their size and of the waiting times between consecutive events. We obtain a generic scaling form which describes crackling noise in materials with different degrees of heterogeneity. The results are in a good agreement with acoustic emission measurements in three-point bending experiments.

Key words: crackling noise, acoustic emission, discrete element model, avalanche, scaling

1. INTRODUCTION

The brittle fracture of materials has two substantially different scenarios depending on the amount of structural disorder: for homogeneous materials such as crystalline solids at the critical stress a single crack is formed which propagates in an unstable manner. However, in materials with a high degree of heterogeneity fracture develops progressively, *i.e.* under an increasing external load first microcracks nucleate at local weaknesses which may then undergo several steps of growth and arrest. Finally macroscopic fracture occurs as the culmination of the gradual accumulation of damage. The nucleation and growth of cracks is accompanied by the emission of elastic waves which can be recorded in the form of acoustic noise. Measuring acoustic emissions (AE) on loaded specimens is the primary source of information on the microscopic dynamics of the fracture of heterogeneous brittle materials (Alava et al., 2006, Deschanel et al., 2009). During the last two decades a large number of AE experiments were carried out which revealed that the energy of acoustic bursts E and the waiting times T between consecutive acoustic events are characterized by power law distributions. The value of the exponents is found to be characteristic for the type of fracture, *i.e.* for ductile fracture the exponents are larger than for brittle breaking since large acoustic bursts are suppressed in ductile materials (Deschanel et al., 2009; Kun et al., 2004).

Very recently the statistical features of acoustic emissions have been analyzed during three-point bending tests of notched concrete specimens. The notch ensures that the formation of microcracks is dominated by strong spatial correlations in a narrow cross section of the specimen. Varying the detection threshold of acoustic signals, for the waiting time distributions $p(T)$ the scaling behaviour $p(T) = Rf(RT)$ was found, where R is the average rate of events during the experiment (Niccolini et al., 2009).

ISSN 1641-8581

The scaling function f proved to be a *gamma* distribution $f(x) = Ax^y\exp(-x/B)$. In Niccolini et al., (2009) the three-point bending experiment was modelled by discretizing the bar in terms of a bundle of fibers. It was a crutial feature of the model that after fiber breakings the load was redistributed equally in the bundle neglecting the spatial correlation of microfractures. Computer simulation of the bending process revealed the same scaling structure of the numerical results as of the experiments, however, for the scaling function f an exponential form was obtained $f(x) \propto \exp(-RT)$. These results demonstrate the importance of the range of stress redistribution and correlations in the statistics of microfractures.

Motivated by these theoretical and experimental findings, in the present paper we investigate the fracture of heterogeneous materials under three-point bending conditions by means of a discrete element model (DEM). Our two-dimensional DEM approach provides a realistic representation of the microstructure of the material, the formation of microcracks, and the emerging complicated stress field naturally accounting for the correlation of microfractures. As a key element of the modelling, a numerical method is proposed to identify bursts of local breakings in discrete element simulations based on temporal and spatial correlations of breaking events.

2. DEM FOR THREE-POINT BENDING

Three-point bending is a standard engineering test where a bar shaped specimen is clamped at the two ends and a point load is applied in the middle perpendicular to the longer axis of the bar. Under an increasing load the bar bends and finally breaks due to a crack which appears in the middle along the load direction. Besides its engineering importance, three-point bending experiments provide an excellent opportunity to study the propagation of a single crack in a disordered environment. Recently, we have worked out a two-dimensional dynamical model of deformable, breakable granular solids applying randomly shaped convex polygons to describe grains (D'Addetta et al., 2002, Behera et al., 2005). The initial set of polygons is obtained by the Voronoi tessellation of a square from which specimens of appropriate shapes can be cut out. The average polygon size l_p sets the characteristic length scale of the model system. The polygons are considered to be rigid bodies which can overlap when pressed against each other. We introduce a repulsive force between the overlapping particles proportional to the overlap area (D'Addetta et al., 2002, Behera et al., 2005). To capture the elastic behavior of solids we connect the unbreakable, undeformable polygons (grains) by elastic beams. The beams can be elongated, compressed, sheared and bent so that they exert forces and torques on the polygons to which they are attached.

In the simulations a bar shaped specimen is considered with an aspect ratio 1:5 corresponding to the experimental standards (see figure 1). In order to make a realistic representation of three-point loading, the three loading plates are realized by additional polygonal elements, *i.e.* squares in figure 1 with side length $S = 5l_p$ much smaller than the longer side $L = 1000l_p$ of the bar $S << L$. These loading plates interact with the particles of the bar via the overlap force, however, no beams are coupled to them. Strain controlled loading of the bar is implemented in such a way that the two loading plates at the bottom are fixed while the third one on the top is moved vertically downward in figure 1 with a constant speed v_0. The moving plate overlaps the boundary polygons on the top of the bar which results in an increasing loading force. Simulations were carried out with a constant value of v_0 selected to allow for an efficient damping of the elastic waves and to ensure a reasonable CPU time for the computations. In order to simplify the numerical measurements on crack propagation, we introduce a "weak" line in the middle of the bar in such a way that solely those beams are allowed to break which connect the two sides of the line.

The beams, modeling cohesive forces between grains, can be broken according to a physical breaking rule, which takes into account the stretching and bending of the connections

$$\left(\frac{\varepsilon}{\varepsilon_{th}}\right)^2 + \frac{\max(|\Theta_1|,|\Theta_2|)}{\Theta_{th}} \geq 1 \qquad (1)$$

Here ε denotes the longitudinal deformation of a beam, while Θ_1 and Θ_2 are bending angles at the two beam ends. The breaking rule Eq. (1) contains two parameters ε_{th}, Θ_{th} controlling the relative importance of the stretching and bending breaking modes, respectively. The time evolution of the polygonal solid is obtained by solving the equations of motion of the individual polygons. At each iteration step we evaluate the breaking criterion Eq. (1) and remove those beams which fullfill the condition. (For more details of the model construction see D'Addetta et al., (2002)).

The breaking parameters ε_{th}, and Θ_{th} of beams are stochastic variables in the model, i.e. they are sampled from probability density functions $p(\varepsilon_{th})$ and $p(\Theta_{th})$. The Weibull distribution provides a comprehensive description of the stochastic fracture strength of materials, hence, for both threshold values the Weibull form is prescribed

$$p_{\lambda,m}(x) = \frac{m}{\lambda}\left(\frac{x}{\lambda}\right)^{m-1} e^{-\left(\frac{x}{\lambda}\right)^{m}} \qquad (2)$$

where x denotes the two breaking thresholds ε_{th}, Θ_{th}. The Weibull distribution has two parameters: λ sets the characteristic scale of threshold values while the exponent m determines the scatter of the variable. Increasing the value of the exponent m the width of the Weibull distribution Eq. (2) decreases and converges to the delta function in the limit $m \to \infty$. Varying the scale parameters λ_ε and λ_Θ of the breaking thresholds the relative importance of stretching and bending can be controlled in the breaking process. For clarity in the present paper we only investigate the two limiting cases of beam breaking dominated by pure stretching and bending with the parameter settings $\lambda_\varepsilon = 0.05$, $\lambda_\Theta = 100$, and $\lambda_\varepsilon = 100$, $\lambda_\Theta = 1$, respectively. The Weibull exponents were changed in the range $1 \le m \le 50$ for both threshold distributions. We note that due to the randomness of the polygons, besides the strength disorder of beams there is also structural disorder in the system.

can be characterized numerically by measuring the force F acting on the moving plate at the top of the sample as a function of time t. (Note that the deflection of the bar is proportional to t.) Figure 1(b) presents the force-time curve obtained for a sample with the Weibull exponent $m = 2$ in the stretching limit.

It can be seen that the macroscopic response is linear all the way up to catastrophic failure, where the force drops suddenly. This drop becomes more and more drastic as we increase the brittleness of the sample by increasing the value of m. At the beginning of the loading process, the smooth oscillations about the linear in the constitutive curve arise due to elastic waves generated by the loading plate. As the force approaches its maximum, the curve becomes more and more noisy due to internal damage being accumulated in the form of microcracks nucleating throughout the breakable interface. It can be observed in figure 1(b) that after the maximum, the force drops rather drastically, however, the failure is not totally abrupt. The sharp drop-down of the force is followed by stable crack propagation where the crack gradually advances until the sample falls apart. We characterize the degree of brittleness of the sample and its dependence on the amount of threshold disorder by measuring the accumulated damage prior to the maximum of $F(t)$ as a function of the Weibull exponent m. Figure 2(a) shows the damage parameter D of the model, defined as the fraction of beams broken before a single crack starts propagating, for the stretching and bending limits, as a function of the Weibull exponent m. It can be observed that the curves can be very well fitted with the functional form

$$D(m) = C + dm^{-\mu} \qquad (3)$$

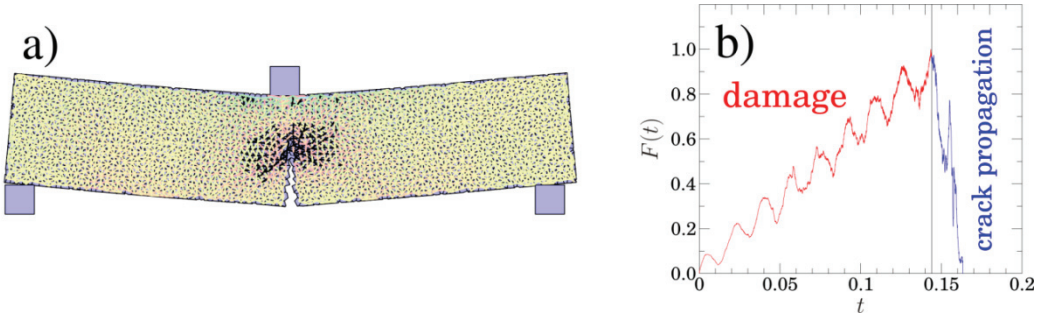

Fig. 1. *(a) Three-point bending of a bar composed of polygonal particles. The particles are coupled by elastic beams which are colored according to the longitudinal deformation (yellow: nearly unstressed beams; red and black: elongated beams; blue and green: compressed beams). Beams are allowed to break solely along the center line of the bar. A relatively small sample is presented to have a clear view on the details of the model construction. The two loading plates at the bottom are fixed while the third one on the top moves downward. (b) Force as a function of time during the loading process. Oscillations occur due to elastic waves generated by the loading process. After the peak the decreasing part of F(t) curve indicates stable crack propagation where our analysis is focused.*

3. MACROSCOPIC RESPONSE

In our strain controlled three-point bending experiment the mechanical response of the material

where both C and μ proved to be different for the stretching and bending limits. Discretizing the weak interface of the sample by a parallel bundle of springs and assuming equal stress redistribution after spring breaking, a power law form can be obtained analytically for the damage parameter $D \propto m^{-1}$with a unique exponent. The higher value of the measured exponents $\mu = 1.9 \pm 0.1$ *(stretching)* and $\mu = 1.5 \pm 0.1$ *(bending)* is the consequence of the strain gradient in the load direction, which was completely neglected in the analytic calculations.

crack. The load redistribution may give rise to additional breakings resulting in a correlated trail of breaking events which are analogous to acoustic signals measured in experiments. In order to identify bursts of local breakings we introduce a correlation time t_{corr}: if the time difference of two consecutive beam breakings occurring at times t_i and t_{i+1} is smaller than the correlation time $t_{i+1} - t_i < t_{corr}$ the two breakings are considered to belong to the same burst. The value of t_{corr} was set to $t_{corr} = 10\Delta t$ for which t_{corr} $10^5 t_{corr} < t_{tot}$ holds, where t_{tot} is the total

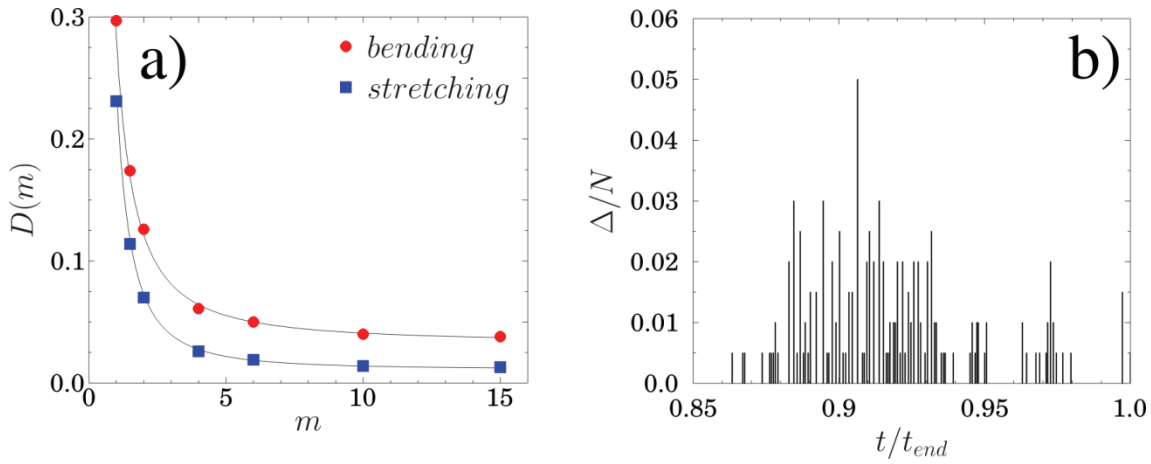

Fig. 2. *(a) Damage accumulated up to the peak of F(t) as a function of the Weibull exponent m. The curves can be very well fitted with the functional form Eq. (3). (b) Time series of bursts in a single fracture simulation. For all the simulations the number of beams N along the interface was set to N = 200. At the beginning of the loading process, for a considerable time no breaking occurs, most of the breaking events appear at larger deflections beyond the peak of the constitutive curve (see figure 1(b)). Hence, we magnify the final section of the bending process.*

Note that in the limit of high m, the non-zero value of C in figure 2(a) can be attributed to the structural disorder in the sample.

Perfectly brittle failure of the bar would be characterized by a linear behaviour of $F(t)$ up to the maximum without any damaging which is then followed by an abrupt breaking. Our simulation results demonstrate that varying the amount of threshold disorder we can control the degree of brittleness of the DEM sample from highly (but not perfectly) brittle to quasi-brittle. It is a very interesting question how the degree of brittleness affects the properties of crackling noise.

4. CRACKLING NOISE DURING CRACK PROPAGATION

The low value of the loading speed has the consequence that in each iteration step of the molecular dynamics simulation either no beam breaking occurs or only a single beam breaks. After a local breaking event the stress gets redistributed increasing the stress concentration on the intact elements ahead the duration of the process. The size of bursts Δ is defined as the number of beams breaking during the correlated sequence.

When the amount of disorder is very high $m \to 1$, especially in the bending limit of breakings, it may happen in DEM simulations that very distant beams break within the correlation time, however, without any real correlation. To obtain information on the strength of spatial correlations in an avalanche, we calculate the distance $h_j = |y_j - y_{j+1}|$ between consecutive beam breakings with the positions y_j and y_{j+1} and sum it up inside an avalanche $h = \sum_{j=1}^{\Delta-1} h_j$.

For a strongly correlated avalanche where each consecutive breaking occurs on adjacent beams the ratio of h and of the burst size Δ is close to the characteristic polygone size $h/\Delta \approx l_p$. In order to filter out avalanches dominated by random coincidences we introduce a threshold value for this ratio, i.e. those avalanches for which $h/\Delta > 2l_p$ are removed from the statistics. Figure 2(b) presents the size of bursts

identified by our method in a single fracture simulation at the time of their appearance.

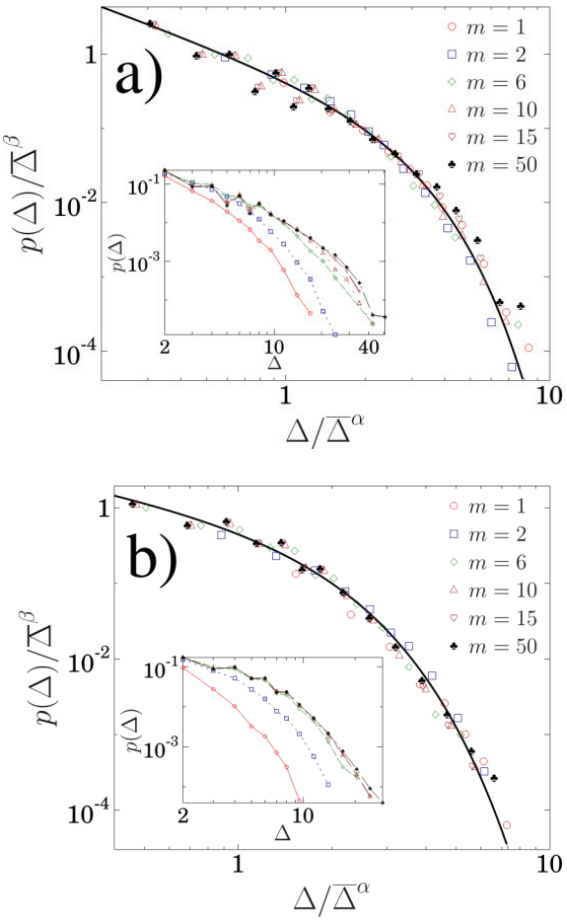

Fig. 3. *Avalanche size distributions for the absolute stretching (a) and bending (b) limits varying the value of the Weibull exponent* m*. The insets present the original distributions while in the main panels scaling plots are shown. The excellent data collapse was obtained by rescaling the distributions with the average burst size according to Eq. (4).*

We determined numerically the size distribution of bursts $p(\Delta)$ varying the amount of disorder in the failure thresholds. The size distribution obtained at different values of the Weibull exponent is presented in the insets of figure 3 (a) and (b) for the absolute stretching and bending limits, respectively. It is interesting to note that increasing the Weibull exponent m, i.e. decreasing the amount of disorder, the bursts get larger but the functional form does not change. For small bursts a power law behavior is obtained followed by a rapidly decreasing cutoff regime. The main panels of figure 3 demonstrate that using the average burst size $\overline{\Delta}$ as a scaling variable, the burst size distributions $p(\Delta)$ obtained at different m values can be collapsed on a master curve. The data collapse implies the scaling structure

$$p(\Delta) = \overline{\Delta}^{\beta} f(\Delta/\overline{\Delta}^{\alpha}) \tag{4}$$

The value of the exponents were determined numerically $\alpha_s = 1.4 \pm 0.05$, $\beta_s = 1.8 \pm 0.07$, and $\alpha_b = 1.4 \pm 0.05$, $\beta_s = 1.8 \pm 0.07$ which provide the best collapse for stretching and bending, respectively. The scaling function f can be very well fitted by the form

$$f(x) = ax^{-\tau} e^{-(x/b)^{\delta}} \tag{5}$$

where the parameter values providing best fit are $a^s_\Delta = 0.55 \pm 0.05$, $\tau^s_\Delta = 1.3 \pm 0.2$, $b^s_\Delta = 2.2 \pm 0.2$, $\delta^s_\Delta = 1.5 \pm 0.3$ *(stretching),* and $a^b_\Delta = 0.85 \pm 0.08$, $\tau^b_\Delta = 0.8 \pm 0.1$, $b^b_\Delta = 1.4 \pm 0.15$, $\delta^b_\Delta = 1.3 \pm 0.3$ *(bending).* The results demonstrate that the growth of the crack is not a smooth process, the slow driving results in a jerky crack propagation which is composed of a large number of discrete steps. The growth steps are sudden outbreaks with a variable length. The correlation of consecutive local breakings leads to a power law functional form. The most interesting outcome of the calculations is that the

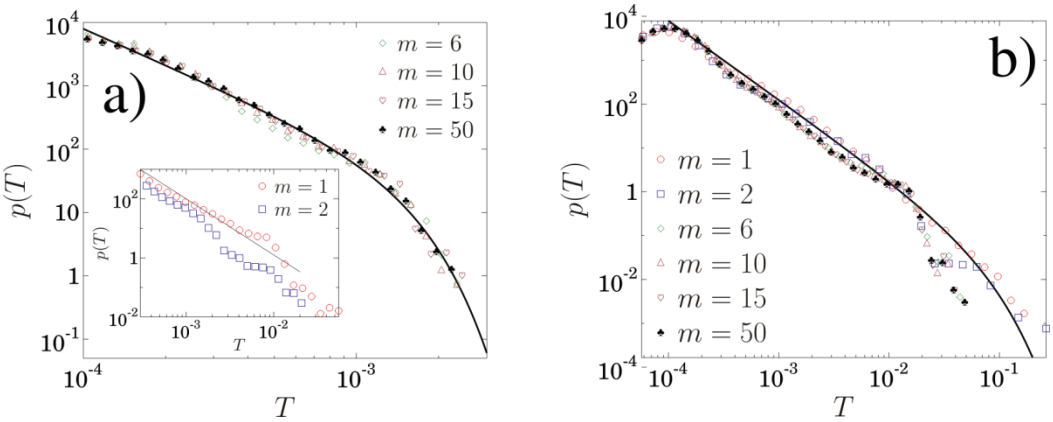

Fig. 4. *Waiting time distributions for absolute stretching (a) and bending limits (b). In (a) the main panel presents curves for low disorder, where the fit was obtained with the exponent* $\tau^s_T = 1.9$*. The inset shows the corresponding curves for high disorder, where a crossover is obtained to a lower exponent* $\tau^s_T = 1.5$*. In the bending limit (b) the amount of disorder only affects the cutoff of the distributions.*

amount of disorder only affects the characteristic scale of bursts but the functional form and the value of the power law exponents remains the same.

It can be observed in figure 2(b) that the bursts are separated by silent periods where no beam breaking occurs. During such periods the crack gets pinned due to some strong beams ahead the crack tip. The advancing loading plate gradually increases the load on the system which reactivates the crack after some waiting time T. It can be seen in figure 2(b) that the duration T of these waiting times can vary in a broad range. In figure 4(a) the waiting time distributions $p(T)$ are presented for the stretching limit separated for high (inset) and low disorder (main panel). It is interesting to note that for low enough disorder (main panel of figure 4(a)) the distributions $p(T)$ are all the same, no dependence on the Weibull exponent could be pointed out. The functional form of $p(T)$ can be very well fitted by the expression Eq. (5) where the value of the exponent $\tau_T^s = 1.9 \pm 0.2$ was obtained. The relatively high value of τ_T^s implies that long waiting times are very rare in the trail of bursts when the material is very brittle. However, in the limit of high disorder $m \to 1$ (see inset of figure 4(a)) waiting times span a broader range and reach an order of magnitude larger values than for the very brittle materials with low disorder. The most remarkable feature of waiting time distributions is that increasing the disorder the exponent of the power law regime changes to the lower value $\tau_T^s \approx 1.5$ coinciding with the recurrence time exponent of one-dimensional random walks. In the absolute bending limit (see figure 4(b)) $p(T)$ has qualitatively the same behaviour as in the stretching limit. Due to the fragility of the system at all Weibull exponents m, the change of disorder only results in a change of the cutoff, however, the value of the exponent of the power law regime is constant $\tau_T^b = 1.8 \pm 0.2$.

5. SUMMARY

The emergence of crackling noise is an ubiquitous phenomenon of the fracture of heterogeneous materials which can also be exploited to monitor the time evolution of the fracture process. Theoretical studies of crackling noise are usually based on stochastic fracture models such as fiber bundles and the fuse model (Alava et al., 2006). As a novel approach to the problem, in the present paper we investigated the properties of crackling noise emerging during the jerky propagation of a crack in three-point bending tests using a discrete element modeling technique. We proposed a numerical method to identify avalanches based on the temporal and spatial correlation of microfractures. Our results demonstrate that for quasi-brittle materials the distribution of the size of bursts and the waiting times between consecutive events are characterized by power law functional forms with an exponential cutoff which obey a generic scaling law. Our numerical results are in a reasonable agreement with recent acoustic emission measurements (Niccolini et al., 2009).

The work is supported by TÁMOP 4.2.1-08/1-2008-003 project. F. Kun acknowledges the Bolyai János fellowship of the Hungarian Academy of Sciences.

REFERENCES

Alava, M.J., Nukala, P., Zapperi, S., 2006, Statistical models of fracture, *Adv. Phys*., 55, 349-476.

Behera, B., Kun, F., McNamara, S., Herrmann, H.J., 2005, Fragmentation of a circular disc by impact on a frictionless plate, *J. Phys.-Cond. Mat*., 17, 2439-2451.

D'Addetta, G.A., Kun, F., Ramm, E., 2002, On the application of a discrete model to the fracture process of cohesive granular materials, *Granular Matter*, 4, 77-92.

Deschanel, S., Vanel,L., Vigier, G., Godin, N., Ciliberto, S., 2006, Statistical properties of microcracking in polyurethane foam under tensile test, influence of temperature and density, *Int. J. Fract*., 140, 87-98.

Kun, F., Lenkey, Gy., Takács, N., Beke, D.L., 2004, Structure of magnetic noise in dynamic fracture, *Phys. Rev. Lett*., 93, 227204-227208.

Niccolini, G., Bosia, F., Carpinteri, A., Lacidogna, G., Manuello, A., Pugno, N., 2009, Self-similarity of waiting times in fracture systems, *Phys. Rev. E*, 80, 026101-026109.

AKUSTYKA PĘKANIA W MODELU ELEMENTÓW DYSKRETNYCH DLA PROPAGACJI POJEDYNCZEGO PĘKNIĘCIA

Streszczenie

W pracy badano odgłos pękania występujący podczas propagacji pojedynczego pęknięcia w próce poddawanej trzypunktowemu zginaniu, symulowanemu za pomocą metody elementów dyskretnych (ang. Discrete element method – DEM). Analiza czasowych i przestrzennych zależności lokalnego pękania wykazała, że pęknięcie postępuje przez rozdzielenie, co charakteryzuje się prawem potęgowym opisującym rozmiar szczelin oraz czasy przerw między kolejnymi etapami pękania. Opracowano ogólną postać skalowania, które opisuje odgłos pękania w materiałach o różnym stopniu niejednorodności. Uzyskane wyniki są zgodne z pomiarami emisji akustycznej w próbie trzypunktowego zginania.

Received: October 3, 2010
Received in a revised form: October 25, 2010
Accepted: October 25, 2010